Modern Physics Letters B
Vol. 34, No. 12 (2020) 2050117 (13 pages)

DOI: 10.1142/S0217984920501171

Lumps, breathers, rogue waves and interaction solutions to a $(3+1)$-dimensional Kudryashov–Sinelshchikov equation

Xianglong Tang

School of Computer Science and Software Engineering, East China Normal University, Shanghai 200062, China

Yong Chen*

School of Mathematical Sciences, Shanghai Key Laboratory of PMMP, East China Normal University, Shanghai 200062, China
Department of Physics, Zhejiang Normal University, Jinhua 321004, China
ychen@sei.ecnu.edu.cn

Received 13 August 2019
Revised 8 October 2019
Accepted 11 November 2019
Published 5 March 2020

Utilizing the Hirota bilinear method, the lump solutions, the interaction solutions with the lump and the stripe solitons, the breathers and the rogue waves for a (3 + 1)-dimensional Kudryashov–Sinelshchikov equation are constructed. Two types of interaction solutions between the lumps and the stripe solitons are exhibited. Some different breathers are given by choosing special parameters in the expressions of the solitons. Through a long wave limit of breathers, the lumps and rogue waves are derived.

Keywords: Hirota bilinear method; interaction solution; breather; rogue wave; (3 + 1)-dimensional Kudryashov–Sinelshchikov equation.

1. Introduction

The nonlinear evolution equations have been used to describe the propagation of the waves in bubbly liquids, such as the Korteweg–de Vries (KdV) equation,[1] the Burgers equation,[2] the Burgers–Korteweg–de Vries equation[1] and so on. A mixture of liquid and gas bubbles can be considered as a classical example of a classic nonlinear medium. The propagation of the waves in bubbly liquids is one of the important problems worthy of investigation. Recently, Kudryashov and Sinelshchikov developed a nonlinear partial differential equation for describing the propagation of

*Corresponding author.

waves in a mixture of the liquid and gas bubbles in the 3D case.[3] Tu *et al.* obtained its exact solutions through Bäcklund transformation (BT).[4] As the exact solutions of the nonlinear evolution equations can provide much physical information and more insight into the physical aspects of the problems, it is important to obtain the exact solutions to nonlinear evolution equations.

To find exact solutions to nonlinear evolution equations, a series of methods have been proposed and developed, such as the Inverse Scattering transformation (IST),[5–7] BT,[8,9] symmetry approach,[10–13] Darboux transformation (DT),[14–17] Hirota bilinear method[18–23] and so on.

Among these methods, the Hirota bilinear method is a popular way to construct the exact solutions to nonlinear evolution equations. The Hirota bilinear method can be applied to construct various types of exact solutions, such as the lump solutions, interaction solutions, breathers and rogue waves. Lumps are rational function solutions and localized in all directions in the space. Rogue waves are another kind of rational function solutions, which have an amplitude more than twice the background waves and appear from nowhere and disappear without a trace. Rogue waves were observed in deep water,[24] oceans,[25] fiber optics[26] and so on. Breathers are localized in one certain direction with a periodic structure. In addition, breathers serving as the potential prototype for the rogue waves in a lot of physics fields are worthy of investigation.[27] In recent years, the Hirota bilinear method is applied to construct the lump and the interaction solutions between the lump and the stripe solitons.[28–36] In addition, the lump solutions and rogue waves can be obtained through a long wave limit of breathers.[37,38]

In this paper, we consider a (3 + 1)-dimensional Kudryashov–Sinelshchikov equation[39]

$$(u_t + \alpha u u_x + \gamma u_{xxx})_x + d u_{yy} + e u_{zz} = 0\,, \tag{1}$$

where $u = u(x, y, z, t)$ is a differentiable function and α, γ, d, e are arbitrary constants. Equation (1) can describe the liquid containing gas bubbles neglecting the viscosity of the liquid. Equation (1) is a deformed equation of the equation proposed by Kudryashov and Sinelshchikov.[3] Equation (1) is a much common nonlinear evolution equation for describing the waves in bubbly liquids and many well-known nonlinear evolution equations can be derived from Eq. (1). When $d = 0$, $e = 0$, $\alpha = 6$, $\gamma = 1$, Eq. (1) is reduced to the KDV equation.[40] When $e = d$, Eq. (1) is reduced to a generalized (3 + 1)-dimensional KP equation.[41]

For Eq. (1), Chukkol constructed the traveling wave solutions by using a modified tanh–coth method[39] and Zhou obtained the multi-solitons, breathers and elastic interaction solutions.[42] In order to study the wave propagation in bubbly fluid flow in more depth and consider complex situation, in this paper, we construct different types of breathers, as well as the inelastic interaction solutions of Eq. (1).

The paper is organized as follows. In Sec. 2, two types of interaction solutions between the lump and the stripe solitons are derived and their dynamics behaviors are analyzed. In Sec. 3, three kinds of breathers are derived and their dynamics behaviors are shown graphically. In Sec. 4, through a long wave limit of breathers, the lump and the rogue wave solution are derived and the dynamics behaviors of the rogue wave are shown graphically. Section 5 is the conclusion.

2. Interaction Solutions

According to the transformation

$$u = \frac{12\gamma}{\alpha}(\ln f)_{xx}\,. \tag{2}$$

Equation (1) is converted into the bilinear form

$$(D_x D_t + \gamma D_x^4 + dD_y^2 + eD_z^2)f \cdot f = 0\,, \tag{3}$$

where the Hirota bilinear differential operator D_n^m is defined by

$$\begin{aligned} &D_x^m D_y^n (f(x,y)\cdot g(x',y')) \\ &\quad = \left(\frac{\partial}{\partial x} - \frac{\partial}{\partial x'}\right)^m \left(\frac{\partial}{\partial y} - \frac{\partial}{\partial y'}\right)^n f(x,y)g(x',y')|_{x=x',y=y'}\,. \end{aligned} \tag{4}$$

Case 1. Interaction solution between lump soliton and one stripe soliton

In order to obtain the interaction solution between the lump and one stripe soliton, we assume the function f in the bilinear form Eq. (3) is the following form:

$$\begin{aligned} &f = g^2 + h^2 + kl + a_{11}\,, \quad g = a_1 x + a_2 y + a_3 z + a_4 t + a_5\,, \\ &h = a_6 x + a_7 y + a_8 z + a_9 t + a_{10}\,, \quad l = \mathrm{e}^{k_1 x + k_2 y + k_3 z + k_4 t}\,, \end{aligned} \tag{5}$$

where $a_i (1 \le i \le 11)$, $k_j (1 \le i \le 4)$ and k are arbitrary parameters. By substituting Eq. (5) into Eq. (3) and through a direct computation, the parameters are given by

$$\begin{aligned} &a_1 = 0\,, \quad a_3 = 0\,, \quad a_{10} = 0\,, \quad a_4 = \frac{6a_7\gamma a_6 {k_1}^2}{a_2}\,, \quad a_8 = \frac{a_6 k_3}{k_1}\,, \\ &a_9 = -\frac{3a_6 {a_2}^2 \gamma {k_1}^4 - 3{a_7}^2\gamma {k_1}^4 + {a_2}^2 e {k_3}^2}{{a_2}^2 {k_1}^2}\,, \quad a_{11} = \frac{{a_6}^2}{{k_1}^2}\,, \quad d = \frac{-3\gamma {a_6}^2 {k_1}^2}{{a_2}^2}\,, \\ &k_2 = \frac{a_7 k_1}{a_6}\,, \quad k_4 = -\frac{{a_2}^2\gamma {k_1}^4 - 3{a_7}^2\gamma {k_1}^4 + {a_2}^2 e {k_3}^2}{{a_2}^2 k_1}\,. \end{aligned} \tag{6}$$

By substitution of Eq. (6) into Eq. (5), a class of functions consisting of two quadratic functions and an exponential function are obtained as follows:

$$\begin{aligned} f = &\left(a_2 y + a_3 z + \frac{6a_8 a_6 \gamma k_1^2 t}{a_3} + a_5\right)^2 \\ &+ \left(a_6 x + a_7 y + a_8 z - \frac{3\gamma a_6 k_1^2 (a_3^2 - a_8^2)t}{a_3^2} + a_{10}\right)^2 \\ &+ \frac{a_6^2}{k_1^2} + k\mathrm{e}^{k_1 x + k_2 y + \frac{k_1 a_8 z}{a_6} - \frac{\gamma k_1^3 (a_3^2 - 3a_8^2)t}{a_3^2}}\,. \end{aligned} \tag{7}$$

By substitution of Eq. (7) into Eq. (2), and choosing $a_2 = 2$, $a_3 = 1$, $a_5 = 0$, $a_6 = 1$, $a_7 = 1$, $a_8 = 1$, $a_{10} = 0$, $k = 2$, $k_1 = -2$, $k_2 = 0$, $e = 1$, $\gamma = -1$ and $\alpha = -12$, the solution of Eq. (1) is changed into

$$u = \frac{2 + 8e^{16t-2x-2z}}{(-24t + 2y + z)^2 + (x + y + z)^2 + \frac{1}{4} + 2e^{16t-2x-2z}} - \frac{(2x + 2y + 2z - 4e^{16t-2x-2z})^2}{((-24t + 2y + z)^2 + (x + y + z)^2 + \frac{1}{4} + 2e^{16t-2x-2z})^2}\,. \tag{8}$$

The dynamic behaviors and corresponding density plots are shown in Fig. 1. From Fig. 1, the inelastic interaction between the lump soliton and one stripe wave can be noted. When $t = -\frac{1}{3}$, before the fusion, the lump and the stripe wave have not yet begun to interact, the speed of the stripe wave is $v_s = 8$ and the speed of the lump soliton is $v_l = \sqrt{2}$. The direction of v_s is along the x-axis and the direction of v_l is along the vector $(-1, 1)$. The amplitude of the stripe wave is $u = 1.012$ at $x = -5.670$ and the amplitude of the lump soliton is $u = 8$ at $(-4, 4)$. It is obvious that the amplitude of the lump soliton is much larger than the amplitude of the stripe wave before the fusion occurs. When $t = 0$, the inelastic interaction between two waves begins to occur and the energy of the lump soliton begins to transfer into the stripe wave. In this time, the amplitude of the lump is $u = 3.855$ and the amplitude of the stripe wave is $u = 1.063$. As the energy of the lump begins

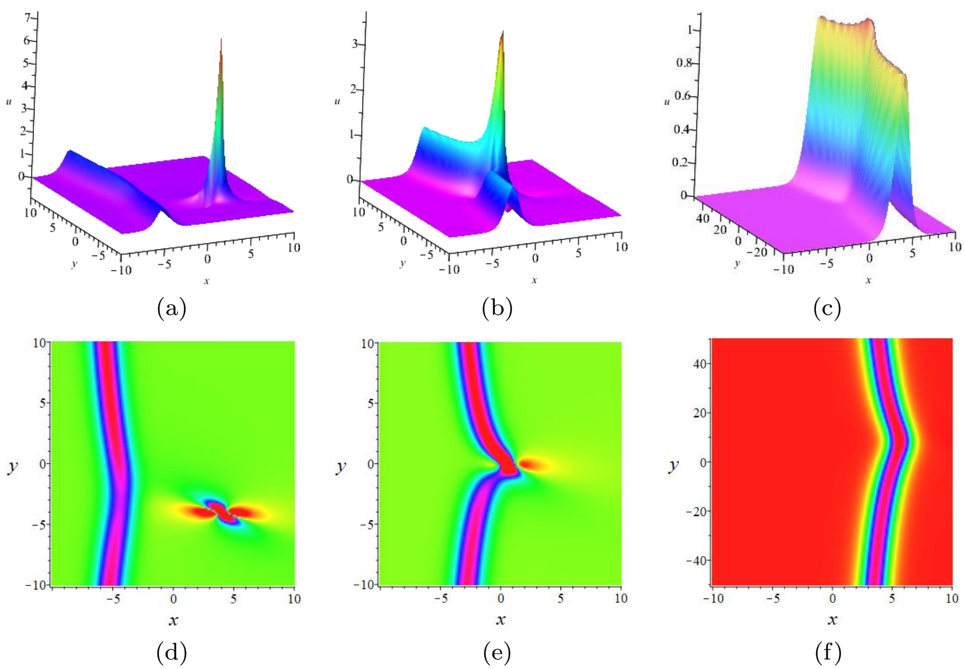

Fig. 1. (Color online) The time evolution of the interaction solution and corresponding density plots by choosing (a) $t = -\frac{1}{3}$, (b) $t = 0$ and (c) $t = \frac{1}{3}$ in the (x, y) plane.

to transfer into the stripe wave, the amplitude of the lump decreases rapidly after the collision. The shapes of the two waves have changed since the beginning of the fusion. When $t = \frac{1}{3}$, the stripe wave has completely swallowed the lump soliton. After the interaction, the two waves fuse with each other and the common speed is the speed of the stripe soliton $v_c = 8$.

Case 2. Interaction solution between lump soliton and two stripe solitons

In order to obtain the interaction solution between the lump and two resonance stripe solitons, we assume the function f in the bilinear form Eq. (3) is the following form:

$$\begin{aligned} &f = g^2 + h^2 + k\cosh(l) + a_{11}, \quad l = k_1 x + k_2 y + k_3 z + k_4 t, \\ &g = a_1 x + a_2 y + a_3 z + a_4 t + a_5, \quad h = a_6 x + a_7 y + a_8 z + a_9 t + a_{10}, \end{aligned} \tag{9}$$

where $a_i (1 \le i \le 11)$, $k_j (1 \le i \le 4)$ and k are arbitrary parameters. By substituting Eq. (9) into Eq. (3) and through a direct computation, the parameters are given by

$$\begin{aligned} &a_{11} = \frac{k^2 {k_1}^4 + 4{a_1}^4}{4{a_1}^2 {k_1}^2}, \quad a_4 = \frac{3a_1\gamma {k_1}^2 {a_2}^2 - {a_7}^2}{{a_7}^2}, \quad a_6 = 0, \quad a_9 = \frac{6a_1 a_2 \gamma {k_1}^2}{a_7}, \\ &d = \frac{-3{a_1}^2\gamma {k_1}^2}{{a_7}^2}, \quad e = 0, \quad k_2 = \frac{a_2 k_1}{a_1}, \quad k_4 = \frac{3\gamma {k_1}^3 {a_2}^2 - {a_7}^2}{{a_7}^2}. \end{aligned} \tag{10}$$

By substitution of Eq. (10) into Eq. (9), a class of functions consisting of two quadratic functions and a hyperbolic function are obtained as follows:

$$\begin{aligned} f = {} & \left(a_1 x + a_2 y + a_3 z + \frac{3a_1\gamma k_1^2(a_2^2 - a_7^2)t}{a_7^2} + a_5\right)^2 \\ & + \left(a_7 y + a_8 z + \frac{6a_1 a_2 \gamma k_1^2 t}{a_7} + a_{10}\right)^2 \\ & + k\cosh\left(k_1 x + \frac{a_2 k_1 y}{a_1} + k_3 z + \frac{\gamma k_1^3(3a_2^2 - a_7^2)t}{a_7^2}\right) + \frac{k^2 k_1^4 + 4a_1^4}{4a_1^2 k_1^2}. \end{aligned} \tag{11}$$

By substitution of Eq. (11) into Eq. (2), and choosing $a_1 = 1$, $a_2 = -\frac{1}{5}$, $a_3 = 1$, $a_5 = 0$, $a_7 = 1$, $a_8 = 1$, $a_{10} = 0$, $k = 2$, $k_1 = 1$, $k_3 = 1$, $\gamma = 4$ and $\alpha = 48$, the solution of Eq. (1) is changed into

$$\begin{aligned} u = {} & \frac{2 + 2\cosh\left(x - \frac{1}{5}y + z - \frac{88}{25}t\right)}{\left(x - \frac{1}{5}y + z - \frac{288}{25}t\right)^2 + \left(y + z - \frac{24}{5}t\right)^2 + 2\cosh\left(x - \frac{1}{5}y + z - \frac{88}{25}t\right) + 2} \\ & - \frac{\left(2x - \frac{2}{5}y + 2z - \frac{576}{25}t + 2\sinh\left(x - \frac{1}{5}y + z - \frac{88}{25}t\right)\right)^2}{\left(\left(x - \frac{1}{5}y + z - \frac{288}{25}t\right)^2 + \left(y + z - \frac{24}{5}t\right)^2 + 2\cosh\left(x - \frac{1}{5}y + z - \frac{88}{25}t\right) + 2\right)^2}. \end{aligned} \tag{12}$$

The interaction solution between the lump and two resonance stripe solitons is obtained. For the solution in Eq. (12), the asymptotic property of the lump soliton and the two resonance stripe solitons are analyzed. By taking x and y as constants, it can be found that

$$
\begin{aligned}
\lim_{t\to\pm\infty}\frac{g^2}{h^2} &= \lim_{t\to\pm\infty}\frac{\left(x-\frac{1}{5}y+z-\frac{288}{25}t\right)^2}{\left(y+z-\frac{24}{5}t\right)^2}=\frac{144}{25}\,,\\
\lim_{t\to\pm\infty}\frac{g^2}{\cosh(l)} &= \lim_{t\to\pm\infty}\frac{\left(x-\frac{1}{5}y+z-\frac{288}{25}t\right)^2}{\cosh\left(x-\frac{1}{5}y+z-\frac{88}{25}t\right)}=0\,,
\end{aligned}
\tag{13}
$$

which implies that when $t\to\pm\infty$, there are only two resonance stripe solitons, and when t is little, the lump soliton is more clear. The dynamic behaviors and corresponding density plots are shown in Fig. 2.

From Fig. 2, the inelastic interaction between the lump and two resonance stripe solitons can be noted. When $t=0$, the lump is just in the middle of the two resonance stripe waves, and because of the interaction, the shapes of the two resonance stripe waves have changed. Furthermore, the amplitude of the lump is 1.0 at $(0,0)$, and the amplitude of the resonance stripe solitons is 0.238 at $x=10$ and $x=-2.05$. It is obvious that the amplitude of the lump is significantly higher than the amplitude of the resonance stripe waves. When $t=\frac{1}{2}$, the lump interacts with one of the resonance stripe waves. Because the energy of the lump begins to transfer into the resonance stripe waves, the amplitude of the lump begins to decrease. At

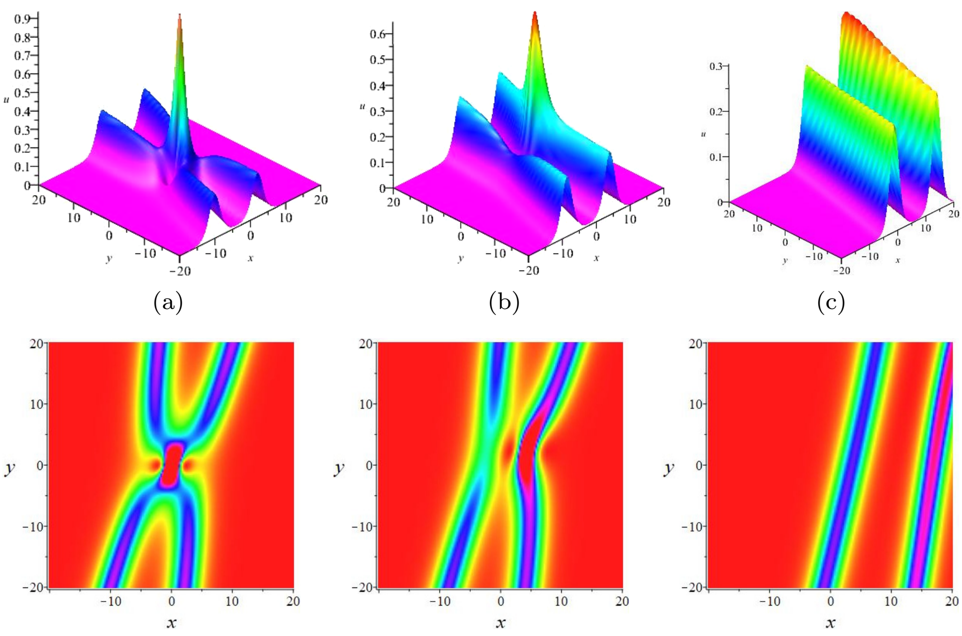

Fig. 2. (Color online) The time evolution and corresponding density plots of the interaction solution by choosing (a) $t=0$, (b) $t=\frac{1}{2}$ and (c) $t=3$ in the (x,y) plane.

this time, the amplitude of the lump is 0.485 at $(6.24, 2.4)$ and the amplitude of the resonance stripe waves is 0.249. When $t = 3$, one of the resonance stripe waves has completely swallowed the lump soliton. Particularly, the two resonance stripe waves always maintain the same speed.

3. Breather Solutions

In this section, we consider three types of breathers, which can be obtained by choosing appropriate parameters on the soliton solutions. We assume the function f in the bilinear form Eq. (3) has the following form:

$$\begin{aligned} f &= 1 + \mathrm{e}^{\eta_1} + \mathrm{e}^{\eta_2} + A_{12}\mathrm{e}^{\eta_1+\eta_2}\,, \\ \eta_i &= k_i(x + p_i y + q_i z + w_i t) + \eta_{0i}\ (i = 1, 2)\,, \end{aligned} \tag{14}$$

where $k_i, p_i, q_i, w_i, \eta_{0i}$ and A_{12} are arbitrary parameters. By substituting Eq. (14) into Eq. (3), the parameters are given by

$$\begin{aligned} A_{12} &= \frac{-3\gamma(k_1 - k_2)^2 + d(p_1 - p_2)^2 + e(q_1 - q_2)^2}{-3\gamma(k_1 + k_2)^2 + d(p_1 - p_2)^2 + e(q_1 - q_2)^2}\,, \\ w_1 &= -dp_1^2 - eq_1^2 - \gamma k_1^2,\ w_2 = -dp_2^2 - eq_2^2 - \gamma k_2^2\,. \end{aligned} \tag{15}$$

Substituting Eq. (15) into Eq. (14) with Eq. (2) and choosing specific values of parameters, three types of breathers can be obtained.

If we set $k_1 = k_2 = \delta_1$, $p_1 = p_2^* = \alpha_1 + i\beta_1$, $\eta_{01} = \eta_{02} = 0$ and q_1 and q_2 are real numbers, one type of the breathers can be obtained. We choose $\delta_1 = \frac{1}{3}$, $\beta_1 = -\frac{3}{5}$, $c_1 = 1$, $c_2 = 2$ and different α_1, then the two (x, y)-periodic breathers and one y-periodic breather are obtained and shown in Fig. 3. Through the observation of Figs. 3(a)–3(c), we find the value of α_1 can change the direction of the breathers but the period of the breathers is not affected.

If we set $k_1 = k_2^* = i\delta_1$, $p_1 = p_2^* = \alpha_1 + i\beta_1$, $q_1 = q_2^* = \rho_1 + i\omega_1$ and $\eta_{01} = \eta_{02} = 0$, one of the breathers can be obtained. We choose $\delta_1 = 1$, $\alpha_1 = 1$, $\beta_1 = -\frac{1}{2}$, $\rho_1 = \frac{1}{5}$,

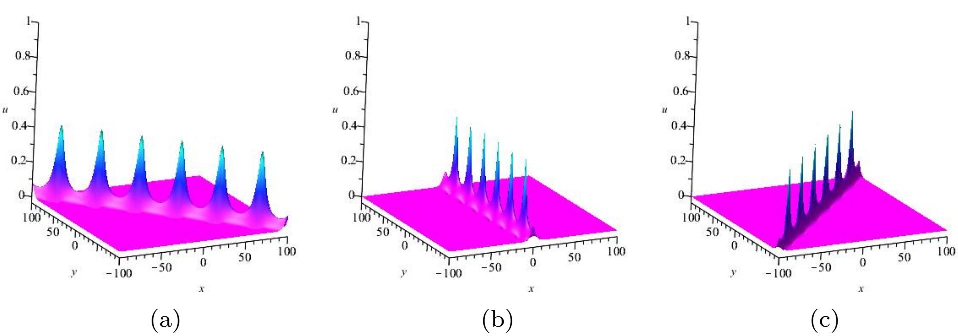

(a) (b) (c)

Fig. 3. (Color online) The 3D plots and corresponding density plots of the breathers by choosing $e = 1$, $d = 2$, $\gamma = 2$, $\alpha = 24$, $t = 0$ and $z = 0$, (a) $\alpha_1 = 1$, (b) $\alpha_1 = 0$ and (c) $\alpha_1 = -1$ in the (x, y) plane.

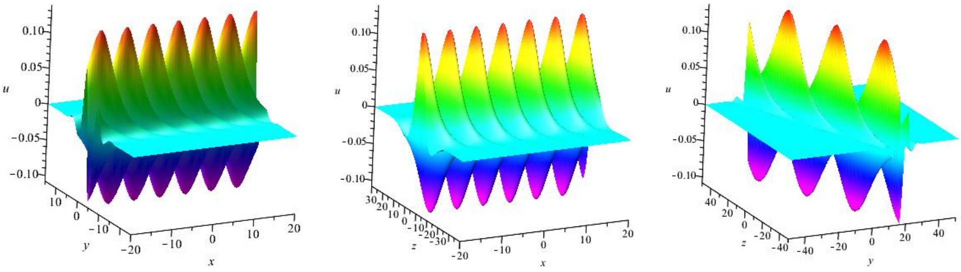

(a) (b) (c)

Fig. 4. (Color online) The 3D plots and corresponding density plots of the breathers by choosing $d = -\frac{1}{2}$, $e = 2$, $\gamma = 1$, $\alpha = 12$ and $t = 0$, (a) in the (x, y) plane, (b) in the (x, z) plane and (c) in the (y, z) plane.

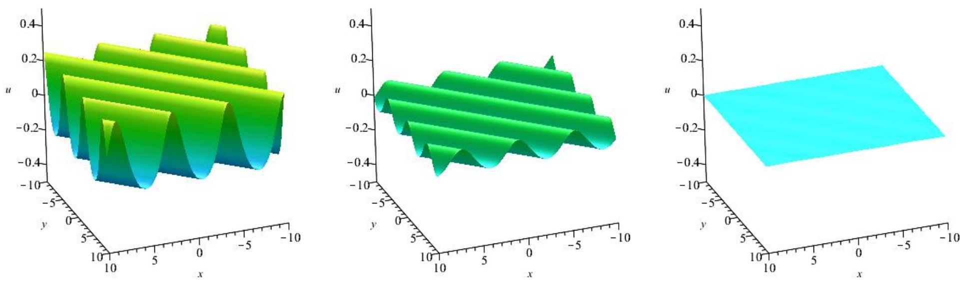

(a) (b) (c)

Fig. 5. (Color online) The time evolution plots of the line breathers in the (x, y) plane by choosing $e = 1$, $d = -1$, $\gamma = 1$, $\alpha = 12$, $z = 0$ and (a) $t = 0$, (b) $t = \frac{1}{5}$ and (c) $t = 1$ in the (x, y) plane.

$\omega_1 = -\frac{1}{5}$, $\eta_{01} = 0$, $\eta_{02} = 0$ and show the solution in Fig. 4 in the (x, y) plane, (x, z) plane and (y, z) plane.

If we set $k_1 = k_2^* = i\delta_1$, $p_1 = p_2 = \alpha_1$, $q_1 = q_2^* = \rho_1 + i\omega_1$ and $\eta_{01} = \eta_{02} = 0$, the line breathers can be obtained. We choose $\delta_1 = 1$, $\alpha_1 = 1$, $\rho_1 = 5$, $\omega_1 = \frac{1}{2}$, and show the solution and dynamic behaviors in Fig. 5. The line breathers are based on a constant background. In addition, they keep parallel and have no interaction with each other. The time evolution plots of the line breathers are shown in Fig. 5. When $t = 0$, the line breathers reach the maximum amplitude. When $t = 0.2$, the amplitude of line breathers has obviously decreased comparing to the amplitude when $t = 0$. When $t = 1$, the breathers has almost retreated back to the constant uniformly.

4. Lump and Rogue Wave Solution

In this section, we construct the lump solution and the rogue wave solution of Eq. (1) through the long wave limit method. Setting the parameters

$$k_1 = l_1\epsilon, \quad k_2 = l_2\epsilon, \quad \eta_{01} = \eta_{02}^* = i\pi \tag{16}$$

into Eq. (15) with Eq. (14), and taking the limit as $\epsilon \to 0$, the function f can be written as

$$f = (\theta_1\theta_2 + \theta_0)l_1 l_2 \epsilon^2 + O(\epsilon^3)\,, \tag{17}$$

where

$$\begin{aligned} \theta_0 &= \frac{12\gamma}{d(p_1 - p_2)^2 + e(q_1 - q_2)^2}\,, \\ \theta_i &= (dp_1^2 + eq_1^2)t - p_1 y - q_1 z - x \ (i = 1, 2)\,. \end{aligned} \tag{18}$$

Substituting Eq. (18) into Eq. (17) with Eq. (2), the solution u can expressed as

$$u = \frac{-12\gamma(\theta_1^2 + \theta_2^2 - 2\theta_0)}{\alpha(\theta_1\theta_2 + \theta_0)^2}\,. \tag{19}$$

Case 1. Lump solution

If we set $p_1 = a_1 + ib_1, q_1 = a_2 + ib_2$, where a_1, a_2, b_1, b_2 are real constants and $a_1 \neq 0$, the lump solution can be obtained. Substituting p_1 and q_1 into Eq. (18) with Eq. (19), the solution u can be rewritten as

$$u = -\frac{24\gamma(g^2 - h^2 + 3\gamma)}{\alpha(g^2 + h^2 - 3\gamma)^2}\,, \tag{20}$$

with

$$\begin{aligned} g &= (b_1^2 d + b_2^2 e)(a_1^2 dt + a_2^2 et - b_1^2 dt - b_2^2 et - a_1 y - a_2 z - x)\,, \\ h &= (b_1^2 d + b_2^2 e)(2a_1 b_1 dt + 2a_2 b_2 et - b_1 y - b_2 z)\,, \end{aligned}$$

where a_1, a_2, b_1, b_2, d, e, α and γ are arbitrary real constants. At any fixed time t, when the $x^2 + y^2 \to +\infty$, the lump solution u in Eq. (20) approaches zero, since the solution u depicts a standard lump structure. Now, we consider the amplitudes and the velocities of the lump solutions in the case that z equals zero. Let the partial derivatives u_x and u_y be zero, the three critical points are obtained at

$$\left(\frac{(a_1^2 b_1 + b_1^3)dt + (2a_1 a_2 b_2 + b_1 b_2^2 - a_2^2 b_1)et + (a_2 b_1 - a_1 b_2)z}{b_1}, \frac{2a_1 b_1 dt + 2a_2 b_2 et - b_2 z}{b_1}\right),$$

$$\left(\frac{\pm 3\sqrt{-\gamma b_1^2(b_1^2 d + b_2^2 e)} - (b_1^3 dt + (a_1^2 dt - a_2^2 et + b_2^2 et + a_2 z)b_1 + 2b_2(eta_2 - \frac{1}{2}z)a_1)(b_1^2 d + b_2^2 e)}{(b_1^2 d + b_2^2 e)b_1}, \right.$$
$$\left. \frac{2a_1 b_1 dt + 2a_2 b_2 et - b_2 z}{b_1}\right),$$

which result in the maximum amplitude is $\frac{-8b_1^2d-8b_2^2e}{\alpha}$, and the minimum amplitude is $\frac{b_1^2d+b_2^2e}{\alpha}$. Therefore, the lump possesses one peak and two valleys. Now, we consider the velocities of the lump in the (x, y) plane. From the extreme points and setting $z = 0$, we know that the lump moves along the route line

$$y = -\frac{2(a_1b_1d + a_2b_2e)x}{b_1^3d + ((-a_2^2 + b_2^2)e + a_1^2d)b_1 + 2b_2a_1a_2e}\,, \tag{21}$$

with the velocities

$$V_x = -\frac{a_1^2b_1d + 2a_1a_2b_2e - a_2^2b_1e + b_1^3d + b_1b_2^2e}{b_1}, \quad V_y = 2a_1b_1d + 2a_2b_2e\,. \tag{22}$$

By setting $a_1 = 1$, $b_1 = 2$, $a_2 = 2$, $b_2 = 1$, $d = -1$, $e = 1$, $\gamma = 1$, $\alpha = 12$, $z = 0$ and $t = 0$ in Eq. (20), the lump solution can be obtained, as shown in Fig. 6(a). When $t = 0$, the maximum amplitude is 4 at $(0, 0)$ and the minimum amplitude is -0.25 at $(-\sqrt{3}, 0)$ and $(\sqrt{3}, 0)$. The lump moves with the velocities ($V_x = 6$, $V_y = 0$).

Case 2. Rogue wave solution

We set $b_2 = 0$ in Eq. (20), the rational solution u in Eq. (20) can be rewritten as

$$u = -\frac{24\gamma(g^2 - h^2 + 3\gamma)}{\alpha(g^2 + h^2 - 3\gamma)^2} \tag{23}$$

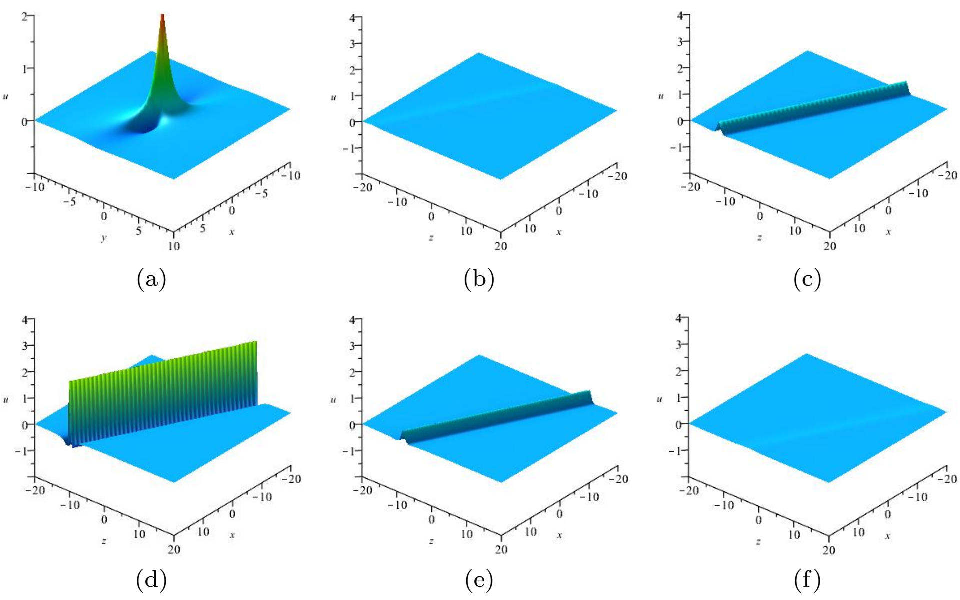

Fig. 6. (Color online) The time evolution and corresponding density plots of the lump and the rogue wave solutions in the (x, z) plane by choosing $d = -1$, $e = 0$, $\gamma = 1$, $\alpha = 12$ and (a) $t = 0$, (b) $t = -2$, (c) $t = -\frac{1}{2}$, (d) $t = 0$, (e) $t = \frac{1}{2}$ and (f) $t = 2$.

with

$$g = b_1^2 d(a_1^2 dt + a_2^2 et - b_1^2 dt - a_1 y - a_2 z - x)\,,$$
$$h = b_1^2 d(2a_1 b_1 dt - b_1 y)\,,$$

which is converted to the line rogue waves possessing a varying amplitude. By setting $a_1 = 1$, $b_1 = 2$, $a_2 = 2$, $d = -1$, $e = 1$, $\gamma = 1$, $\alpha = 12$, the rogue wave solutions are obtained and their dynamic behaviors are shown in Fig. 6. Now, we consider the dynamics of the rogue wave solutions in the case that y equals to zero. Let the partial derivatives u_x and u_z be zero, when $x = (a_1^2 d - b_1^2 d + a_2^2 e)t - a_2 z$, the value of the rogue waves is maximum and the amplitude is $\frac{8}{64t^2+3}$. It shows that the amplitude of the rogue waves reaches the maximum when $t = 0$, and the rogue waves approach the constant background as the $|t| \gg 0$. In Fig. 6, when $t = 0$, the amplitude of the rogue waves reaches the maximum $\frac{8}{3}$. When $t = 0.5$, the amplitude of the rogue waves is $\frac{8}{19}$. When $t = 2$, the amplitude of the rogue waves decreases to $\frac{8}{259}$.

5. Conclusions

In summary, we study the lump solutions, two types of interaction solutions with the lump and the stripe solitons, the breathers, the rogue waves and their dynamics characters to a $(3 + 1)$-dimensional Kudryashov–Sinelshchikov equation. The interaction solution between the lump and one stripe soliton (see Fig. 1) is obtained by utilizing the Hirota bilinear method and combining positive quadratic functions and an exponential function. The interaction solution between the lump and two stripe solitons (see Fig. 2) is constructed by utilizing the Hirota bilinear method and combining positive quadratic functions and a hyperbolic function. The time evolution plots are presented and the inelastic interactions are analyzed, respectively. At first, the lump and the stripe solitons are separated, and then the stripe solitons start to swallow the lump soliton. Finally, the two waves combine into one. Furthermore, three types of breathers (see Figs. 3–5) are constructed by choosing specific parameters on the soliton solutions. The time evolution plots are presented and their dynamic characteristics are analyzed, respectively. Finally, the lump and rogue wave solutions (see Fig. 6) are obtained through a long wave limit of the breathers. These solutions are shown graphically and their dynamic behaviors are analyzed. The line rogue wave arises from a constant background, and then disappears back to the initial background again.

Acknowledgments

The project is supported by the National Natural Science Foundation of China (Nos. 11435005 and 11675054) and Science and Technology Commission of Shanghai Municipality (No. 18dz2271000).

References

1. L. J. van Wijngaarden, *Fluid Mech.* **33** (1968) 465.
2. V. E. Nakoryakov, V. V. Sobolev and I. R. Shreiber, *Fluid Dynam.* **7** (1972) 763.
3. N. A. Kudryashov and D. I. Sinelshchikov, *Phys. Scripta* **85** (2012) 025402.
4. J. M. Tu, S. F. Tian, M. J. Xu, X. Q. Song and T. T. Zhang, *Nonlinear Dynam.* **83** (2016) 1199.
5. M. J. Ablowitz and P. A. Clarkson, *Solitons, Nonlinear Evolution Equations and Inverse Scattering* (Cambridge University Press, Cambridge, 1991).
6. X. E. Zhang and Y. Chen, *Appl. Math. Lett.* **98** (2019) 306.
7. M. J. Ablowitz, B. F. Feng, X. D. Luo and Z. H. Musslimani, *Theor. Math. Phys.* **196** (2018) 1241.
8. C. Rogers and W. K. Schief, *Bäcklund and Darboux Transformations, Geometry and Modern Applications in Soliton Theory*, *Cambridge Texts in Applied Mathematics* (Cambridge University Press, Cambridge, 2002).
9. X. Lu, F. Lin and F. Qi, *Appl. Math. Model.* **39** (2015) 3221.
10. W. X. Ma, *Discrete Contin. Dynam. Syst. Ser. S.* **11** (2018) 707.
11. X. R. Hu and Y. Q. Li, *Appl. Math. Lett.* **51** (2016) 20.
12. B. Ren, *Phys. Scripta* **90** (2015) 065206.
13. S. D. Zhu and J. F. Song, *Appl. Math. Lett.* **83** (2018) 33.
14. L. M. Ling, B. F. Feng and Z. N. Zhu, *Nonlinear Anal. RWA* **40** (2018) 185.
15. T. Xu and Y. Chen, *Commun. Nonlinear Sci.* **57** (2018) 276.
16. C. H. Gu, H. S. Hu and Z. X. Zhou, *Darboux Transformation in Soliton Theory and Geometric Applications* (Shanghai Science and Technology Press, Shanghai, 1999).
17. M. Chen, B. Li and Y. X. Yu, *Commun. Theor. Phys.* **71** (2019) 27.
18. R. Hirota, *The Direct Method in Soliton Theory* (Cambridge University Press, Cambridge, 2004).
19. R. Hirota, *J. Math. Phys.* **14** (1973) 805.
20. L. N. Gao, X. Y. Zhao, Y. Y. Zi, J. Yu and X. Lü, *Comput. Math. Appl.* **72** (2016) 1225.
21. Y. H. Yin, W. X. Ma, J. G. Liu and X. Lü, *Comput. Math. Appl.* **76** (2018) 1275.
22. H. N. Xu, W. Y. Ruan, Y. Zhang and X. Lü, *Appl. Math. Lett.* **99** (2020) 105976.
23. M. D. Chen and B. Li, *Mod. Phys. Lett. B* **31** (2017) 1750298.
24. A. Chabchoub, N. P. Hoffmann and N. Akhmediev, *Phys. Rev. Lett.* **106** (2011) 204502.
25. D. R. Solli, C. Ropers, P. Koonath and B. Jalali, *Nature* **450** (2007) 1054.
26. N. Akhmediev, J. M. Soto-Crespo and A. Ankiewicz, *Phys. Lett. A* **373** (2009) 2137.
27. D. J. Kedziora, A. Ankiewicz and N. Akhmediev, *Phys. Rev. E* **85** (2012) 066601.
28. W. X. Ma, *Phys. Lett. A* **379** (2015) 1975.
29. X. E. Zhang, Y. Chen and Y. Zhang, *Comput. Math. Appl.* **74** (2017) 2341.
30. M. D. Chen, X. Li, Y. Wang and B. Li, *Commun. Theor. Phys.* **67** (2017) 595.
31. W. X. Ma, *East Asian J. Appl. Math.* **9** (2019) 185.
32. P. Wu *et al.*, *Mod. Phys. Lett. B* **32** (2018) 1850106.
33. H. Wang, *Appl. Math. Lett.* **85** (2018) 27.
34. Y. F. Hua, B. L. Guo, W. X. Ma and X. Lü, *Appl. Math. Model.* **74** (2019) 184.
35. J. Wang, H. L. An and B. Li, *Mod. Phys. Lett. B* **33** (2019) 1950262.
36. L. N. Gao, Y. Y. Zi, Y. H. Yin, W. X. Ma and X. Lü, *Nonlinear Dynam.* **89** (2017) 2233.
37. Y. Q. Liu, X. Y. Wen and D. S. Wang, *Comput. Math. Appl.* **77** (2019) 947.
38. C. Qian, J. G. Rao, Y. B. Liu and J. S. He, *Chinese Phys. Lett.* **33** (2016) 110201.

39. Y. B. Chukkol, M. N. B. Mohamad and M. Muminov, *Rom. Rep. Phys.* **2018** (2018) 7452786.
40. V. E. Zakharov and L. D. Faddeev, *Funct. Anal. Appl.* **5** (1971) 18.
41. X. B. Wang, S. F. Tian, H. Yan and T. T. Zhang, *Comput. Math. Appl.* **74** (2017) 556.
42. A. J. Zhou and A. H. Chen, *Phys. Scripta* **93** (2018) 125201.